

Suppressing Spin Qubit Dephasing by Nuclear State Preparation

D. J. Reilly¹, J. M. Taylor², J. R. Petta³, C. M. Marcus¹

M. P. Hanson⁴ and A. C. Gossard⁴

¹ Department of Physics, Harvard University, Cambridge, MA 02138, USA

² Department of Physics, Massachusetts Institute of Technology, Cambridge, MA 02139, USA

³ Department of Physics, Princeton University, Princeton, NJ 08544, USA

⁴ Materials Department, University of California, Santa Barbara, California 93106, USA

Coherent spin states in semiconductor quantum dots offer promise as electrically controllable quantum bits (qubits) with scalable fabrication. For few-electron quantum dots made from gallium arsenide (GaAs), fluctuating nuclear spins in the host lattice are the dominant source of spin decoherence. We report a method of preparing the nuclear spin environment that suppresses the relevant component of nuclear spin fluctuations below its equilibrium value by a factor of ~ 70 , extending the inhomogeneous dephasing time for the two-electron spin state beyond $1 \mu\text{s}$. The nuclear state can be readily prepared by electrical gate manipulation and persists for > 10 s.

Quantum information processing requires the realization of interconnected, controllable quantum two-level systems (qubits) that are sufficiently isolated from their environment that quantum coherence can be maintained for much longer than the characteristic operation time. Electron spins in quantum dots are an appealing candidate system for this application, as the spin of the electron is typically only weakly coupled to the environment compared to the charge degree of freedom [1]. Logical qubits formed from pairs of spins provide additional immunity from collective dephasing, forming a dynamical decoherence-free subspace [2, 3].

Implementing any spin-qubit architecture requires the manipulation [4, 5, 6] and detection [7, 8] of few-electron spin states, as yet only demonstrated in III-V semiconductor heterostructure devices such as gallium arsenide (GaAs), which, in all cases, comprise atoms with nonzero nuclear spin. The nuclear spins of the host lattice couple to electrons via the hyperfine interaction and causes rapid electron spin dephasing. In the GaAs devices presented here, for instance, an ensemble of initialized spin pairs will retain their phase relationship for $T_2^* \sim 15$ ns, consistent with theoretical estimates [9, 10, 11] and previous measurements [4]. The time T_2^* represents an inhomogeneous dephasing time, which can be extended using spin-echo methods [4]. Extending T_2^* by nuclear state preparation reduces the burden of using echo sequences or large field gradients to overcome the fluctuating hyperfine fields when controlling spin qubits.

Proposals to reduce dephasing by nuclear state preparation include complete nuclear polarization [12], state-narrowing of the nuclear distribution [12, 13, 14, 15], and schemes for decoupling the bath dynamics from the coherent evolution of the electron spin using control pulses [16, 17, 18]. These approaches remain largely unexplored experimentally, though recent optical experiments [19] have demonstrated a suppression of nuclear fluctuations in ensembles of self-assembled quantum dots.

We demonstrate a nuclear state preparation scheme in a double quantum-dot system using an electron-nuclear flip-flop pumping cycle controlled by voltages applied to

electrostatic gates. Cyclic evolution of the two-electron state through the resonance between the singlet (S) and $m_s = 1$ triplet (T_+) [20] leads to a 70-fold suppression of fluctuations below thermal equilibrium of the hyperfine field gradient between the dots along the total field direction. It is this component of the hyperfine field gradient that is responsible for dephasing of the two-electron spin qubit formed by S and $m_s = 0$ triplet (T_0) states [4]. Consequently, though the flip-flop cycle generates only a modest nuclear polarization ($< 1\%$), the resulting nuclear state extends T_2^* of the $S-T_0$ qubit from 15 ns to beyond $1 \mu\text{s}$. Once prepared, this non-equilibrium nuclear state persists for ~ 15 s, eventually recovering equilibrium fluctuations on the same time scale as the relaxation of the small induced nuclear polarization. Noting that this recovery time is $\sim 9 - 10$ orders of magnitude longer than typical gate operation times, we propose that occasional nuclear state preparation by these methods may provide a remedy to hyperfine-mediated spin dephasing in networks of interconnected spin qubits.

The double quantum dot is defined in a GaAs/AlGaAs heterostructure with a two-dimensional electron gas (2DEG) 100 nm below the wafer surface (density $2 \times 10^{15} \text{ m}^{-2}$, mobility $20 \text{ m}^2/\text{Vs}$). Negative voltages applied to Ti/Au gates create a tunable double-well potential that is tunnel coupled to adjacent electron reservoirs [see Fig. S1 of Supporting Online Material (SOM)]. A proximal radio-frequency quantum point contact (rf-QPC) senses the charge state of the double dot, measured in terms of the rectified sensor output voltage V_{rf} [21]. Measurements were made in a dilution refrigerator at base electron temperature of 120 mK.

A schematic energy level diagram (Fig. 1A), with (n,m) indicating equilibrium charge occupancies of the left and right dots, shows the three $(1,1)$ triplet states (T_+ , T_0 , T_-) split by a magnetic field \mathbf{B}_0 applied perpendicular to the 2DEG. The detuning from the $(2,0)$ - $(1,1)$ degeneracy, ε , is controlled by high-bandwidth gate voltages pulses. The ground state of $(2,0)$ is a singlet, with the $(2,0)$ triplet out of the energy range of the experiment.

Each confined electron interacts with $N \sim 10^6$ nu-

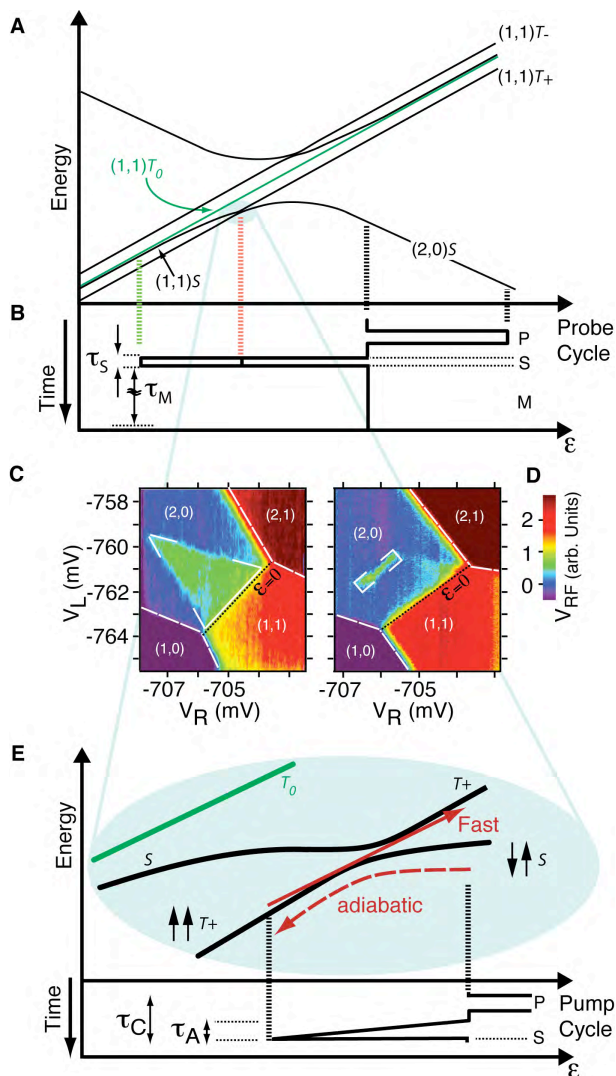


FIG. 1: (A) Schematic of the energy levels of the two-electron system in a magnetic field. Detuning, ε , from the (2,0)-(1,1) charge degeneracy is gate controlled. (B) Gate-pulse sequence used to separately probe the longitudinal, ΔB_n^{\parallel} (green dashed line), and transverse, ΔB_n^{\perp} (red dashed line) components of the Overhauser field difference, depending on the position of the separation point S. (C and D) Time-averaged charge-sensing signal, V_{rf} from the rf-QPC, as a function of gate biases V_L and V_R , showing features corresponding to the singlet mixing with the T_0 (bracketed green triangle in C) and T_+ (bracketed green line segment in D). (E) Schematic view of the $S - T_+$ anticrossing, illustrating the pumping cycle. With each iteration of this cycle, with period $\tau_C = 250$ ns, a new singlet state is taken adiabatically through the $S - T_+$ anticrossing in a time $\tau_A = 50$ ns, then returned nonadiabatically to (2,0) in ~ 1 ns, where the S state is then reloaded.

clei via hyperfine coupling, giving rise to a spatially and temporally fluctuating effective magnetic (Overhauser) field [9, 10, 11, 22]. In the separated (1,1) state, precession rates for the two electron spins depends on their local effective fields, which can be decomposed into an

average field and a difference field. It is useful to resolve $\mathbf{B}_n = (\mathbf{B}_n^{\parallel} + \mathbf{B}_n^{\perp})/2$, the Overhauser part of the total average field, $\mathbf{B}_{\text{tot}} = \mathbf{B}_0 + \mathbf{B}_n$, into components along (B_n^{\parallel}) and transverse (B_n^{\perp}) to \mathbf{B}_{tot} . The difference field, due only to Overhauser contributions, is given by $\Delta \mathbf{B}_n = (\mathbf{B}_n^{\parallel} - \mathbf{B}_n^{\perp})/2$, with components along (ΔB_n^{\parallel}) and transverse (ΔB_n^{\perp}) to \mathbf{B}_{tot} . At large negative ε , where the two electrons are well separated and exchange $J(\varepsilon)$ is negligible, ΔB_n^{\parallel} sets the precession rate between S and T_0 states. At the value of detuning where $J(\varepsilon)$ equals the Zeeman energy $E_Z = g\mu_B B_{\text{tot}}$, (g is the electron g -factor and μ_B is the Bohr magneton) precession between S and T_+ states occurs at a rate set by ΔB_n^{\perp} .

To measure the precession or dephasing of spin pairs in the two dots, a gate-pulse cycle (“probe cycle”) first prepares (P) a singlet state in (2,0), then separates (S) the two electrons into (1,1) for a duration τ_S , then measures (M) the probability of return to (2,0). States that evolve into triplets during τ_S remain trapped in (1,1) by the Pauli blockade, and are detected as such by the rf-QPC charge sensor [4]. Figures 1C and D show the time-averaged charge sensing signal, V_{rf} , as a function of constant offsets to gate biases V_L and V_R , with this pulse sequence running continuously. Setting the amplitude of the S-pulse to mix S with T_0 at large detuning (green dashed line, Fig. 1B) yields the “readout triangle” indicated in Fig. 1C. Within the triangle, V_{rf} is between (2,0) and (1,1) sensing values, indicating that for some probe cycles the system becomes Pauli blocked in (1,1) after evolving to a triplet state. Outside this triangle, alternative spin-independent relaxation pathways circumvent the blockade [23]. For a smaller amplitude S-pulse (red dashed line, Fig. 1B), S mixes with T_+ , also leading to partial Pauli blockade and giving the narrow resonance feature seen in Fig. 1D. The dependence of the $S - T_+$ resonance position on applied field B_0 serves as a calibration, mapping gate voltage V_L (at fixed V_R) into total effective field, B_{tot} , including possible Overhauser fields (Fig. 2A). The charge sensing signal, V_{rf} , is also calibrated using equilibrium (1,1) and (2,0) sensing values to give the probability $1 - P_S$ that an initialized singlet will evolve into a triplet during the separation time τ_S (Fig. 2G). A fit to $P_S(\tau_S)$ (Fig. 2C) yields [11, 22, 24] a dephasing time $T_2^* = \hbar/g\mu_B \langle \Delta B_n^{\parallel} \rangle_{\text{rms}} \sim 15$ ns, where $\langle \dots \rangle_{\text{rms}}$ denotes a root-mean-square time-ensemble average.

We now investigate effects of the electron-nuclear flip-flop cycle (“pump cycle”) (Fig. 1E). Each iteration of the pump cycle moves a singlet, prepared in (2,0), adiabatically through the $S - T_+$ resonance, then returns non-adiabatically to (2,0), where the state is re-initialized to a singlet by exchanging an electron with the adjacent reservoir [20]. In principle, with each iteration of this cycle, a change in the angular momentum of the electron state occurs with a corresponding change to the nuclear system. Iterating the pump cycle at 4 MHz creates a modest nuclear polarization of order 1%, as seen previ-

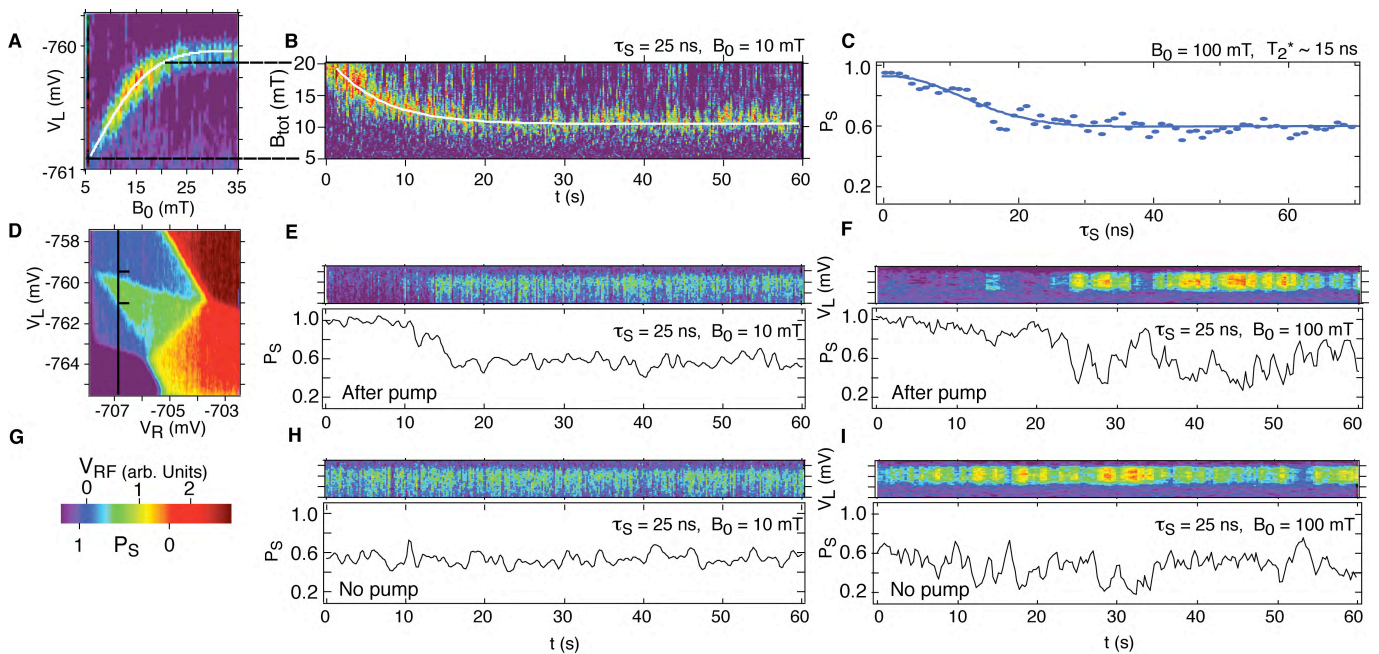


FIG. 2: (A) Position of the $S - T_+$ resonance in V_L as a function of applied magnetic field amplitude B_0 , without prior pump cycle. (B) Evolution of the $S - T_+$ position as a function of time following the pump cycle. Resonance position in gate voltage V_L and converted to B_{tot} via (A). (C) Singlet return probability P_S as a function of τ_S at $B_0 = 100$ mT. Gaussian fit gives an inhomogeneous dephasing time $T_2^* = 15$ ns. (D) Sensor output V_{rf} , as in Fig. 1C, showing triangle that yields P_S . Vertical cut (black line) with brackets shows location of slices in upper panels of (E-I). (E-F) Following the pump cycle, repeated slices across this triangle at the position indicated by the black line in (D) allow a calibrated measure of P_S as it evolves in time, at (E) $B_0 = 10$ mT and (F) $B_0 = 100$ mT. (G) shows the calibration between the sensing signal V_{rf} and singlet return probability P_S . (H and I) are control experiments showing slices across the triangle as in (E) and (F), but without a prior pump cycle.

ously [20]. The pump cycle was always iterated for more than 1 s, and no dependence on pumping time beyond 1 s was observed. What limits the efficiency of the pumping cycle, keeping the polarization in the few-mT regime, is not understood.

Immediately following the pump cycle, the gate-voltage pattern is switched to execute one of two types of probe cycles. The first type of probe cycle starts in (2,0) and makes a short excursion into (1,1) to locate the $S - T_+$ resonance, allowing B_{tot} to be measured via Fig. 2A. Figure 2B shows that the nuclear polarization established by the pumping cycle relaxes over ~ 15 s. The second type of probe cycle starts in (2,0) and makes a long excursion deep into (1,1) to measure $P_S(\tau_S)$ where exchange is insignificant and S and T_0 states are mixed by ΔB_n^{\parallel} . We examine $P_S(\tau_S)$ at fixed τ_S as a function of time after the end of the pump cycle by sampling V_{rf} while rastering V_L across the readout triangle. The black line in Fig. 2D shows the value of V_R with the tick marks indicating the upper and lower limit of the rastering. Slicing through the readout triangle allows P_S to be calibrated within each slice. Remarkably, we find that $P_S(\tau_S = 25$ ns) remains close to unity—that is, the prepared singlet remains in the singlet state after 25 ns of separation—for ~ 15 s following the pump cycle (Figs. 2E and 2F). Note that $\tau_S = 25$ ns exceeds by a factor of ~ 2 the value of T_2^* measured when not preceded by the

pump cycle (Fig. 2C). The time after which P_S resumes its equilibrium behavior, with characteristic fluctuations [24] around an average value $P_S(\tau_S = 25$ ns) = 0.5, is found to correspond to the time for the small ($\sim 1\%$) nuclear polarization to relax (Fig. 2B). Measurements of $P_S(\tau_S = 25$ ns) using the same probe cycle without the preceding pump cycle, shown in Figs. 2H-I, do not show suppressed mixing of the separated singlet state.

Measurement of $P_S(\tau_S)$ as a function of τ_S shows that T_2^* for the separated singlet can be extended from 15 ns to 1 μs , and that this enhancement lasts for several seconds following the pump cycle. These results are summarized in Fig. 3. Over a range of values of τ_S , slices through the readout triangle (as in Figs. 2E) are sampled as a function of time following pumping, calibrated using the out-of-triangle background, and averaged, giving traces such as those in Figs. 3B-E. Gaussian fits yield $T_2^* \sim 1$ μs for 0-5 s after the pump cycle and $T_2^* \sim 0.5$ μs for 10-15 s after the pump cycle. After 60 s, no remnant effect of the pump cycle can be seen, with T_2^* returning to ~ 15 ns, as prior to the pump cycle.

The rms amplitude of longitudinal Overhauser field difference, $\langle \Delta B_n^{\parallel} \rangle_{\text{rms}} = \hbar/g\mu_B T_2^*$ is evaluated using T_2^* values within several time blocks following the pump cycle (using data from Fig. 3A). The observed increase in T_2^* following the pump cycle is thus recast in terms of a suppression of fluctuations of ΔB_n^{\parallel} (Fig. 4A). Similarly,

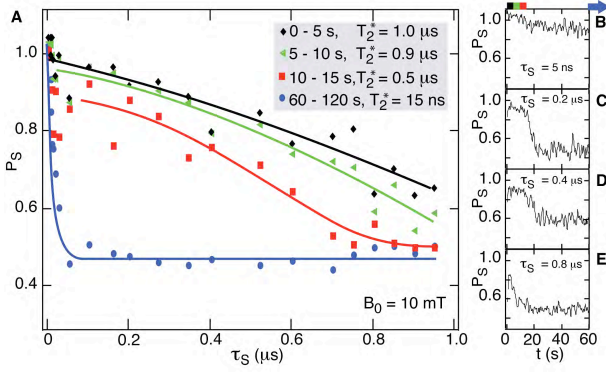


FIG. 3: (A) Singlet return probability P_S as a function of separation time τ_S deep in (1,1) (green dashed line in Fig. 1A), where S mixes with T_0 . P_S averaged within the 0-5 s interval (black), the 5-10 s interval (green), the 10-15 s interval (red), and 60-120 s following the pump cycle, along with gaussian fits. (B-E) P_S as a function of time following the pump cycle ($B_0 = 10$ mT) for fixed $\tau_S = 5$ ns, $\tau_S = 0.2$ μs , $\tau_S = 0.4$ μs and $\tau_S = 0.8$ μs .

the $S - T_+$ mixing rate is used to infer the size of fluctuations of the transverse component of the Overhauser field, $\langle \Delta B_n^\perp \rangle_{\text{rms}}$. Figure 4B shows P_S ($\tau_S = 25$ ns) near the $S - T_+$ resonance. Unlike $S - T_0$ mixing, which is strongly suppressed by the pump cycle, the $S - T_+$ resonance appears as strong as before the pump cycle. This suggests that the energy gap E_n^\perp (Fig. 4E) is not closed by the pump cycle. Note that fluctuations in ΔB_n^\perp produce fluctuations in E_n^\perp , which give the $S - T_+$ anticrossing a width in detuning ε (Fig. 4E). Converting to a width in magnetic field via Fig. 2A, gives the fluctuation amplitude $\langle \Delta B_n^\perp \rangle_{\text{rms}}$ following the pump cycle. Figure 4C shows a representative slice taken from Fig. 4B at the position indicated by the white dashed line. Gaussian fits to each 1 s slice yield mean positions, m , and widths, w , in magnetic field that fluctuate in time, as seen in Fig. 4D. The increase in w for short times ($t < 10$ s) reflects gate-voltage noise amplified by the saturating conversion from gate voltage to effective field at large B_{tot} (see SOM). Beyond these first few seconds, w is dominated by fluctuations of ΔB_n^\perp , but is also sensitive to fluctuations in m that result from fluctuations of B_n^\parallel (see Fig. 4E). (For $t > 10$ s, gate-voltage noise makes a relatively small ($< 10\%$) contribution to the fluctuations). Estimating and removing the contribution due to B_n^\parallel (see SOM) gives an estimate of $\langle \Delta B_n^\perp \rangle_{\text{rms}}$ as a function of time following the pump cycle. These results are summarized by comparing Fig. 4A and 4F: in contrast to the strong suppression of fluctuations in ΔB_n^\parallel following the pump cycle, no corresponding suppression of $\langle \Delta B_n^\perp \rangle_{\text{rms}}$ is observed.

Reducing the cycle rate by a factor ~ 10 reduces, but does not eliminate, the suppression of fluctuations of ΔB_n^\parallel remains evident (see SOM for discussion of dependence of polarization on pump cycle rate). Also, when

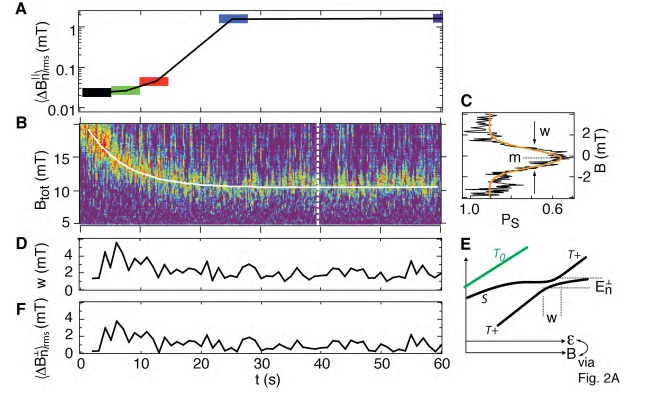


FIG. 4: (A) Amplitude of fluctuating longitudinal Overhauser field, $\langle \Delta B_n^\parallel \rangle_{\text{rms}}$, extracted from T_2^* values at the 5 s intervals in Fig. 3A. (B) $S - T_+$ resonance probed immediately following the pump cycle. Position of the resonance yields B_{tot} and its intensity gives P_S ($B_0 = 10$ mT, $\tau_S = 25$ ns). (C) Slice from (B) at position marked by white dashed line, averaged for 1 s. For each slice a gaussian fit yields the mean position, m , and width, w , of the $S - T_+$ resonance, given in units of magnetic field via Fig. 2(A). (D) Resonance width w as a function of time following the pumping cycle. (E) Schematic of the $S - T_+$ anticrossing showing how fluctuations of E_n^\perp due to ΔB_n^\perp give the resonance a width. (F) Fluctuations in ΔB_n^\perp , as an rms strength $\langle \Delta B_n^\perp \rangle_{\text{rms}}$ in a 1 s slice.

the pump cycle is substituted by a cycle that rapidly brings the singlet into resonance with T_0 , deep in (1,1), effectively performing multiple fast measurements of ΔB_n^\parallel , no subsequent effect on $S - T_0$ mixing is observed. This demonstrates that it is transitions involving S and T_+ , rather than S and T_0 , that lead to the suppression of nuclear field gradient fluctuations.

The observation that an adiabatic electron-nuclear flip-flop cycle will suppress fluctuations of the nuclear field gradient has been investigated theoretically [25, 26]. These models explain some but not all of the observed phenomenology described here, and it is fair to say that a complete physical picture of the effect has not yet emerged. Other nuclear preparation schemes arising from various hyperfine mechanisms, not directly related to the specific pump cycle investigated here, have also been addressed theoretically in the recent literature [27, 28].

Control of spin qubits in the presence of time-varying equilibrium Overhauser gradients require complex pulse sequences [4] or control of sizable magnetic field gradients [2, 29]. Suppressing fluctuations of ΔB_n^\parallel by a factor of order 100, as demonstrated here using nuclear state preparation, leads to an improvement in control fidelity of order 10^4 , assuming typical control errors, which scale as $(\Delta B_n / \Delta B_n^\parallel)^2$ for low-frequency noise. We further anticipate generalizations of the present results using more than two confined spins that allow arbitrary gradients in nuclear fields to be created by active control of Overhauser coupling.

We thank L. DiCarlo and A. C. Johnson for technical contributions and W. Coish, F. Koppens, D. Loss, and A. Yacoby for useful discussions. This work was

supported in part by ARO/IARPA, DARPA, and NSF-NIRT (EIA-0210736). Research at UCSB supported in part by QuEST, an NSF Center.

-
- [1] D. Loss, D. DiVincenzo, *Phys. Rev. A* **57**, 120 (1998).
 [2] J. Levy, *Phys. Rev. Lett.* **89**, 147902 (2002).
 [3] J. M. Taylor et al., *Nature Physics (London)* **1**, 177 (2005).
 [4] J. R. Petta et al., *Science* **309**, 2180 (2005).
 [5] F. H. L. Koppens et al., *Nature (London)*, **442**, 766 (2006).
 [6] K. C. Nowack, F. H. L. Koppens, Yu. V. Nazarov, L. M. K. Vandersypen., *Science*, **318**, 1430 (2007).
 [7] J. M. Elzerman et al., *Nature (London)*, **430**, 431 (2004).
 [8] S. Amasha et al., *Phys. Rev. Lett.* **100**, 046803 (2008).
 [9] S. I. Erlingsson, Y. V. Nazarov, V. I. Fal'ko, *Phys. Rev. B* **64**, 195306 (2001).
 [10] A. V. Khaetskii, D. Loss, L. Glazman, *Phys. Rev. Lett.* **88**, 186802 (2002).
 [11] I. A. Merkulov, A. L. Efros, M. Rosen, *Phys. Rev. B* **65**, 205309 (2002).
 [12] A. Imamoglu, E. Knill, P. Zoller, *Phys. Rev. Lett.* **91**, 017402 (2003).
 [13] D. Klauser, W. A. Coish, D. Loss, *Phys. Rev. B* **73**, 205302 (2006).
 [14] G. Giedke, J. M. Taylor, D. D'Alessandro, M. D. Lukin, and A. Imamoglu, *Phys. Rev. A* **74**, 032316 (2006).
 [15] Dimitrije Stepanenko, Guido Burkard, Geza Giedke, Atac Imamoglu, *Phys. Rev. Lett.* **96**, 136401 (2006).
 [16] K. Khodjasteh, D. A. Lidar, *Phys. Rev. Lett.* **95**, 180501 (2005).
 [17] Wenxian Zhang, V. V. Dobrovitski, Lea F. Santos, Lorenza Viola, and B. N. Harmon, *Phys. Rev. B* **75**, 201302(R) (2007).
 [18] Wang Yao, Ren-Bao Liu, L. J. Sham, *Phys. Rev. Lett.* **98**, 077602 (2007).
 [19] A. Grelich, et al., *Science*, **317**, 1896 (2007).
 [20] J. R. Petta, et al., *Phys. Rev. Lett.* **100**, 067601 (2008).
 [21] D. J. Reilly, C. M. Marcus, M. P. Hanson, A. C. Gossard, *App. Phys. Lett.* **91**, 162101 (2007).
 [22] J. M. Taylor, et al., *Phys. Rev. B* **76**, 035315 (2007).
 [23] A. C. Johnson et al., *Nature (London)*, **435**, 925 (2004).
 [24] D. J. Reilly, et al., arXiv:0712.4033 (2007).
 [25] G. Ramon, X. Hu, *Phys. Rev. B* **75**, 161301(R) (2007).
 [26] W. M. Witzel. S. D. Sarma, arXiv:0712.3065 (2007).
 [27] H. Christ, J. I. Cirac, G. Giedke, *Phys. Rev. B* **75**, 155324 (2007).
 [28] J. Danon, Y. V. Nazarov, *Phys. Rev. Lett.* **100**, 056603 (2008).
 [29] L.-A. Wu, D. A. Lidar, *Phys. Rev. Lett.* **88**, 207902 (2002).